

Ferrocenylselenoether and its Cuprous Cluster Modified TiO₂ as Visible-light Photocatalyst for Synergistic Transformation of N-Cyclic Organics and Cr (VI)

Zhuo Yang^a, Jinshan Wang^a, Aimin Li^b, Chao Wang^{a,c}, Wei Ji^{a,*}, Elísabet Pires^c, Wenzhong Yang^a, Su Jing^{a,*}

^a School of Chemistry and Molecular Engineering, Nanjing Tech University, Nanjing 211816, China. Email: buffycomji@njtech.edu.cn (W. Ji), sjing@njtech.edu.cn (S. Jing)

^b State Key Laboratory of Pollution Control and Resource Reuse, School of the Environment, Nanjing University, Nanjing 210023, China

^c Instituto de Síntesis Química y Catálisis Homogénea, CSIC-Universidad de Zaragoza, Pedro Cerbuna 12, E-50009 Zaragoza, Spain.

Preparation of L0 and fcSe

Figure S1. Crystallographic structure of L0.

Figure S2. ^1H NMR spectrum of L0.

Figure S3. HRMS spectrum of L0.

Figure S4. ^1H NMR spectrum of fcSe.

Figure S5. HR MS spectrum of fcSe.

Figure S6. High-resolution XPS spectrum of Ti 2p in fcSe@TiO₂.

Figure S7. TEM images of fcSe@TiO₂ nanoparticles and size distribution.

Figure S8. TEM images of [Cu₂I₂(fcSe)₂]_n@TiO₂ nanoparticles and size distribution.

Figure S9. FTIR spectra of TiO₂, fcSe, fcSe@TiO₂ and [Cu₂I₂(fcSe)₂]_n@TiO₂.

Figure S10. Nitrogen adsorption-desorption isotherms of fcSe@TiO₂ (blue) and [Cu₂I₂(fcSe)₂]_n@TiO₂ (red).

Figure S11. The first derivative of the Tauc Plot curve for fcSe@TiO₂ and [Cu₂I₂(fcSe)₂]_n@TiO₂.

Figure S12. Transformation efficiency of (a) fcSe@TiO₂, (b) [Cu₂I₂(fcSe)₂]_n@TiO₂ for TC and Cr(VI) in multiple catalytic cycles.

Figure S13. TEM images of fcSe@TiO₂ nanoparticles and size distribution after five catalytic cycles.

Figure S14. TEM images of [Cu₂I₂(fcSe)₂]_n@TiO₂ nanoparticles and size distribution after five catalytic cycles.

Figure S15. FTIR spectra of TiO₂, fcSe, fcSe@TiO₂ and [Cu₂I₂(fcSe)₂]_n@TiO₂ after five cycles.

Figure S16. The fluorescence change of SOSG in response to ¹O₂ generated in the [Cu₂I₂(fcSe)₂]_n@TiO₂ system with $\cdot\text{O}_2^-$ scavenger p-BQ (red line) or TEMPOL (blue line).

Figure S17. The spectrum of the Xenon Lamp MC-PF300C.

Table S1. Crystallographic data for the L0.

Table S2. Selected bond lengths (Å) and bond angles (°) for L0.

Table S3. Zeta potentials and Z-average hydrodynamic diameters of fcSe@TiO₂ and [Cu₂I₂(fcSe)₂]_n@TiO₂ at different pH.

Table S4. TC photocatalytic degradation efficiency comparison of **fcSe@TiO₂** and **[Cu₂I₂(fcSe)₂]_n@TiO₂** with other representative systems.

Table S5. LC-MS spectra of degradation products.

Table S6. Evaluation of **fcSe@TiO₂** and **[Cu₂I₂(fcSe)₂]_n@TiO₂** in the visible light photo-degradation of representative N-cyclic organics.

References

Preparation of **L0** and **fcSe**

All starting materials were analytical grade reagents and purchased from Aladdin or Source Leaf, and used without further purification unless otherwise specified. TiO₂ was commercial P25 (75% anatase, 25% rutile). 1,2,3-Triseleno[3]ferrocenophane **fcSe**₃ (**fc** = [Fe(η^5 -C₅H₄)(η^5 -C₅H₄)]) was prepared according to literature method¹.

L0: **fcSe**₃ (0.426 g, 1 mmol) and NaBH₄ (0.378 g, 10 mmol) were added into anhydrous ethanol (150 mL) under nitrogen atmosphere. The reaction was performed at 0 °C for 30 min, then at 25 °C for 2 h. A THF solution of methyl 4-(bromomethyl)benzoate (0.458 g, 2 mmol) was added, and the reaction was carried out at 25 °C for 24 h. The solid precipitation was obtained by evaporation under reduced pressure, and was treated with water (50 mL) and extracted with dichloromethane (3×50 mL). The extract was dried over magnesium sulfate, evaporated to dryness. The yellowish solid 1,1'-bis[1-(methyl-4-benzoic acid methyl ester)-seleno]ferrocene (**L0**) was obtained by elution with petroleum ether/ethyl acetate (15:1 v/v). Yield 0.457 g (68%). ¹H NMR (400 MHz, CDCl₃, δ): 7.89, 7.87, 7.11, 7.09 (m, 8H, -ArH), 4.16, 4.09 (dd, 8H, -fcH), 3.91 (s, 4H, -Se-CH₂-) 3.79 (s, 6H, -CH₃). ESIMS: 642.8 ([M+H]⁺).

KOH (0.310 g, 5.5 mmol) was added to ethanol (150 mL) solution of **L0** (0.450 g, 0.7 mmol), then the mixture was left to react at 80 °C for 2 h. Part of the solvent was removed by evaporation under reduced pressure, then treated with dichloromethane (50 mL) and extracted with water (3×50 mL). Concentrated hydrochloric acid was added dropwise to the aqueous phase to adjust the acidity to pH=1.0. The yellow precipitation was collected to obtain the target product 1,1'-bis((4-carboxybenzyl)seleno)ferrocene (**fcSe**). Yield 0.381g (86%). ¹H NMR (400 MHz, DMSO-d₆, δ): 12.84 (s, -COOH), 7.78, 7.76 (m, 8H, -ArH), 4.20, 4.09 (dd, 8H, -fcH), 3.87 (s, 4H, -Se-CH₂-). ESIMS: 614.9 ([M+H]⁺).

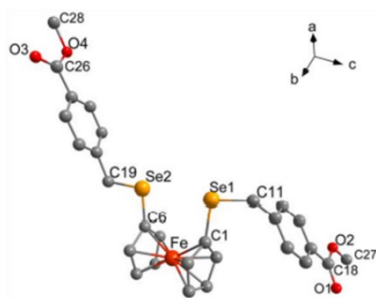


Figure S1. Crystallographic structure of **L0**.

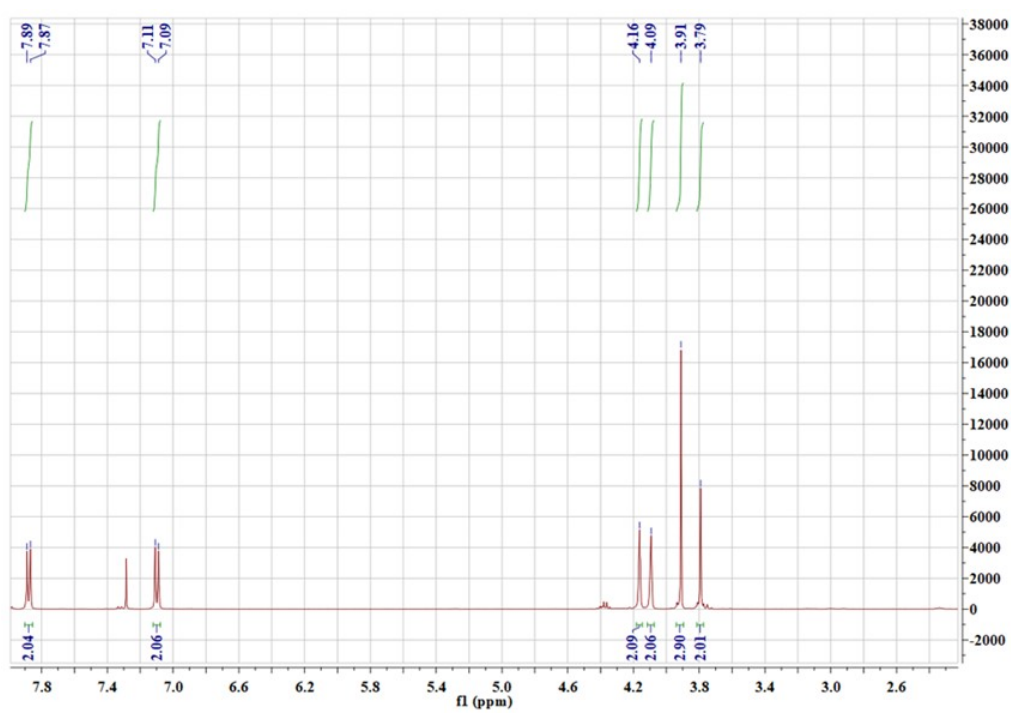
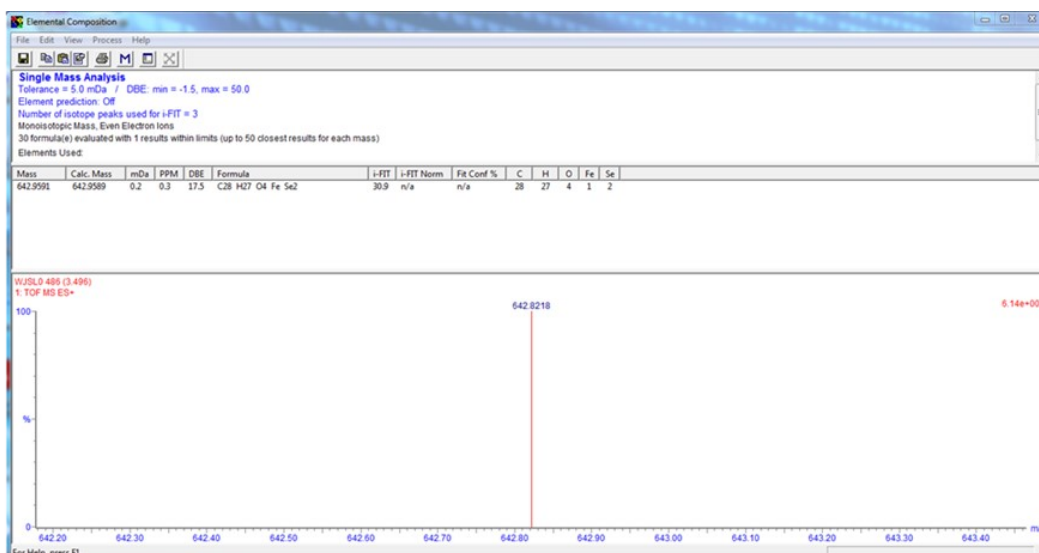


Figure S2. ^1H NMR spectrum of **L0**.



Elemental Composition Report

Page 1

Single Mass Analysis

Tolerance = 5.0 mDa / DBE: min = -1.5, max = 50.0

Element prediction: Off

Number of isotope peaks used for i-FIT = 3

Monoisotopic Mass, Even Electron Ions

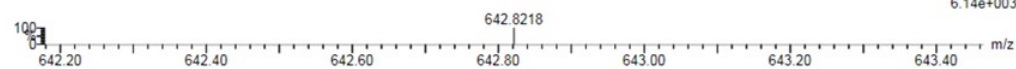
30 formula(e) evaluated with 1 results within limits (up to 50 closest results for each mass)

Elements Used:

C: 24-30 H: 22-28 O: 2-6 Fe: 0-2 Se: 0-2

WJSL0 486 (3.496)

1: TOF MS ES+



Minimum:

Maximum: 5.0 10.0 -1.5 50.0

Mass	Calc. Mass	mDa	PPM	DBE	i-FIT	Norm	Conf (%)	Formula
------	------------	-----	-----	-----	-------	------	----------	---------

642.9591	642.9589	0.2	0.3	17.5	30.9	n/a	n/a	C28 H27 O4 Fe Se2
----------	----------	-----	-----	------	------	-----	-----	-------------------

Figure S3. HRMS spectrum of L0.

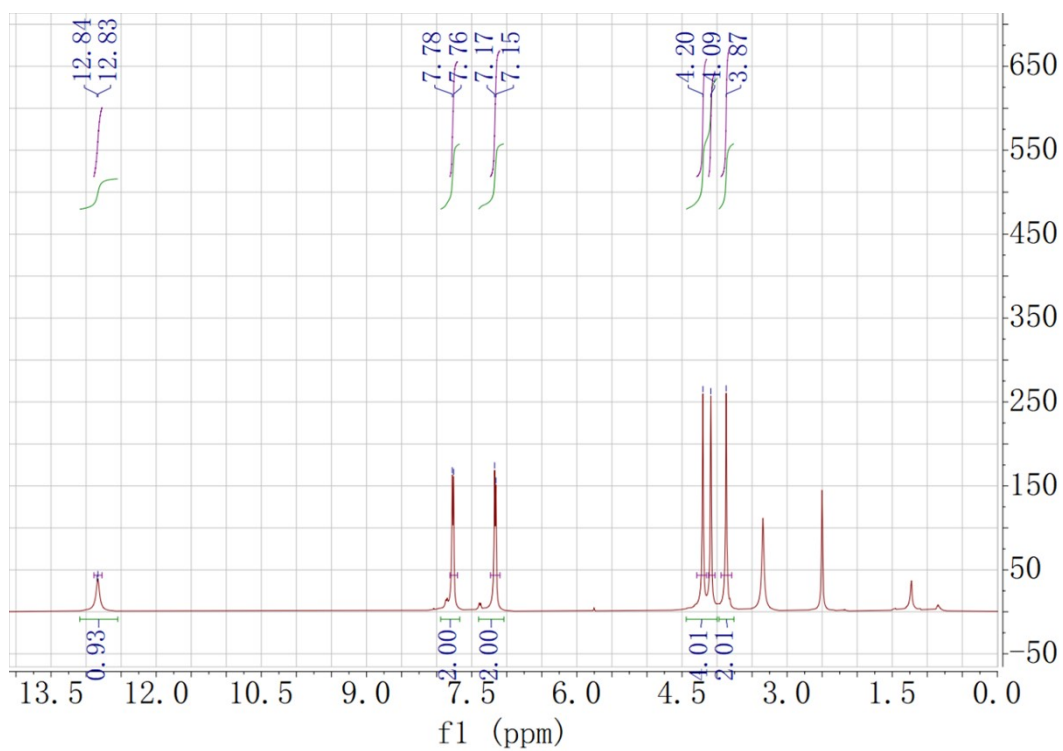
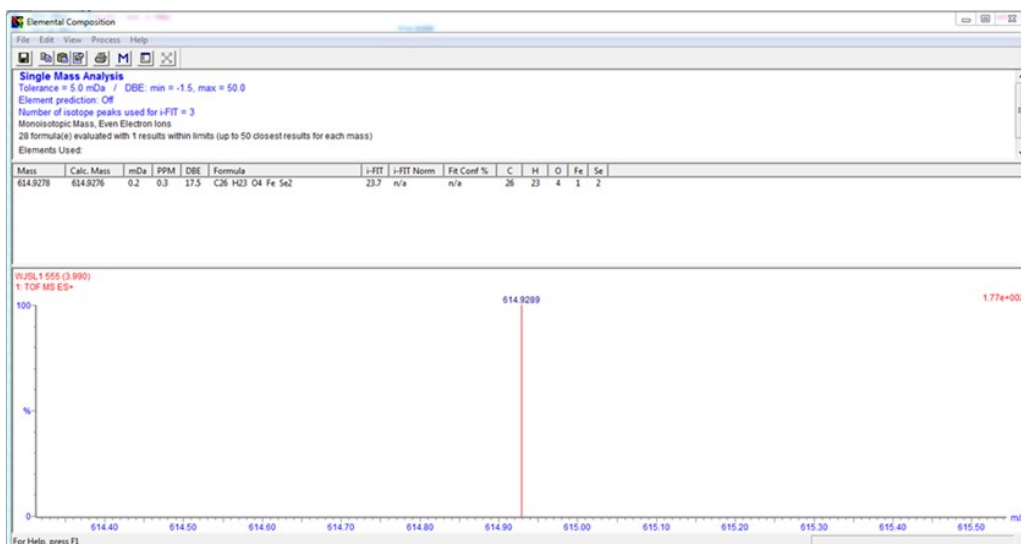


Figure S4. ^1H NMR spectrum of fcSe .



Elemental Composition Report

Page 1

Single Mass Analysis

Tolerance = 5.0 mDa / DBE: min = -1.5, max = 50.0

Element prediction: Off

Number of isotope peaks used for i-FIT = 3

Monoisotopic Mass, Even Electron Ions

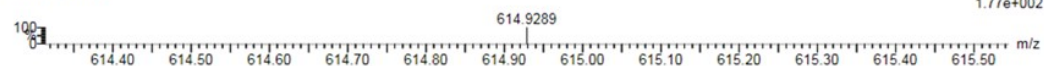
28 formula(e) evaluated with 1 results within limits (up to 50 closest results for each mass)

Elements Used:

C: 24-30 H: 22-28 O: 2-6 Fe: 0-2 Se: 0-2

WJSL1 555 (3 990)

1: TOF MS ES+



Minimum:

Maximum: 5.0 10.0 -1.5 50.0

Mass	Calc. Mass	mDa	PPM	DBE	i-FIT	Norm	Conf (%)	Formula
614.9278	614.9276	0.2	0.3	17.5	23.7	n/a	n/a	C ₂₆ H ₂₃ O ₄ Fe Se ₂

Figure S5. HRMS spectrum of fcSe.

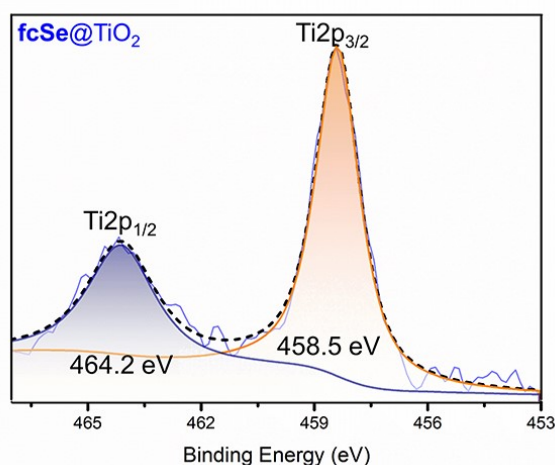


Figure S6. High-resolution XPS spectrum of Ti 2p in fcSe@TiO₂.

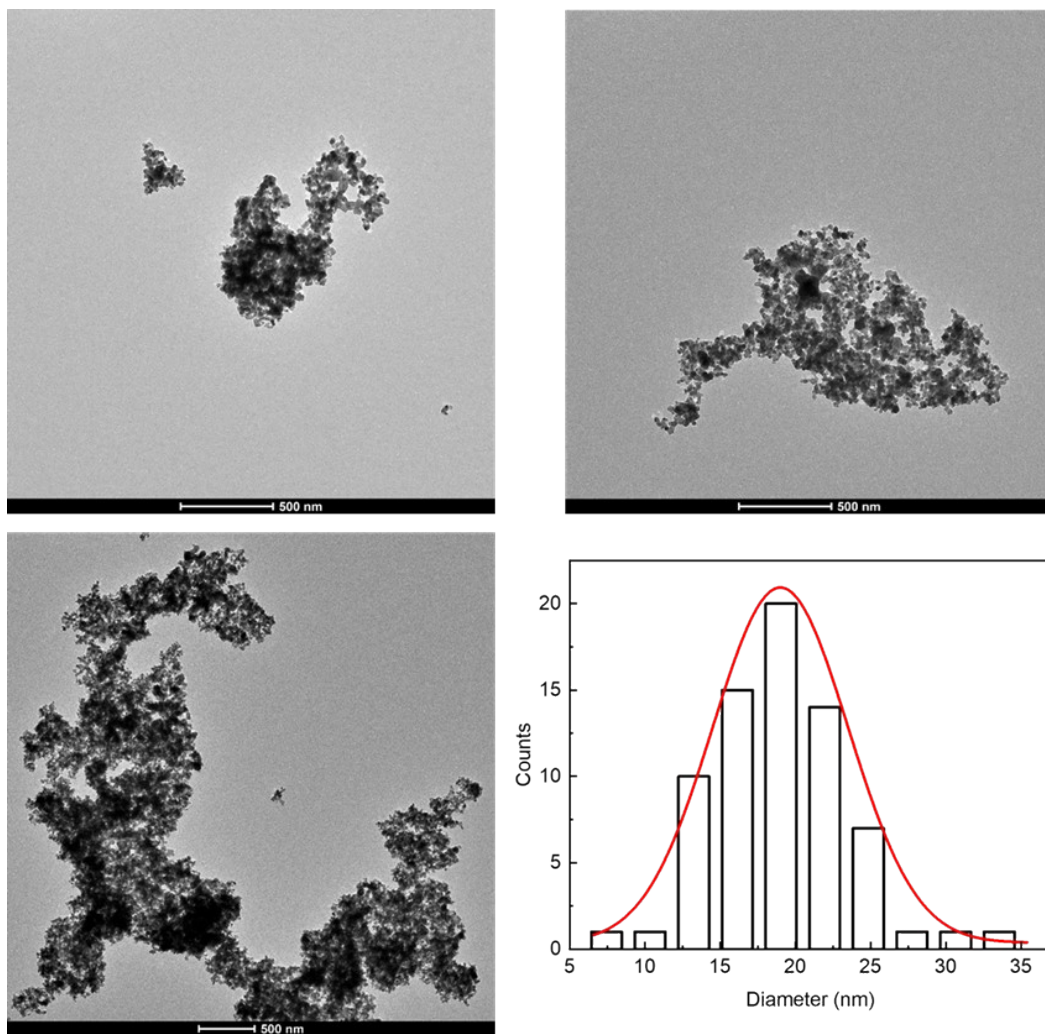


Figure S7. TEM images of fcSe@TiO_2 nanoparticles and size distribution.

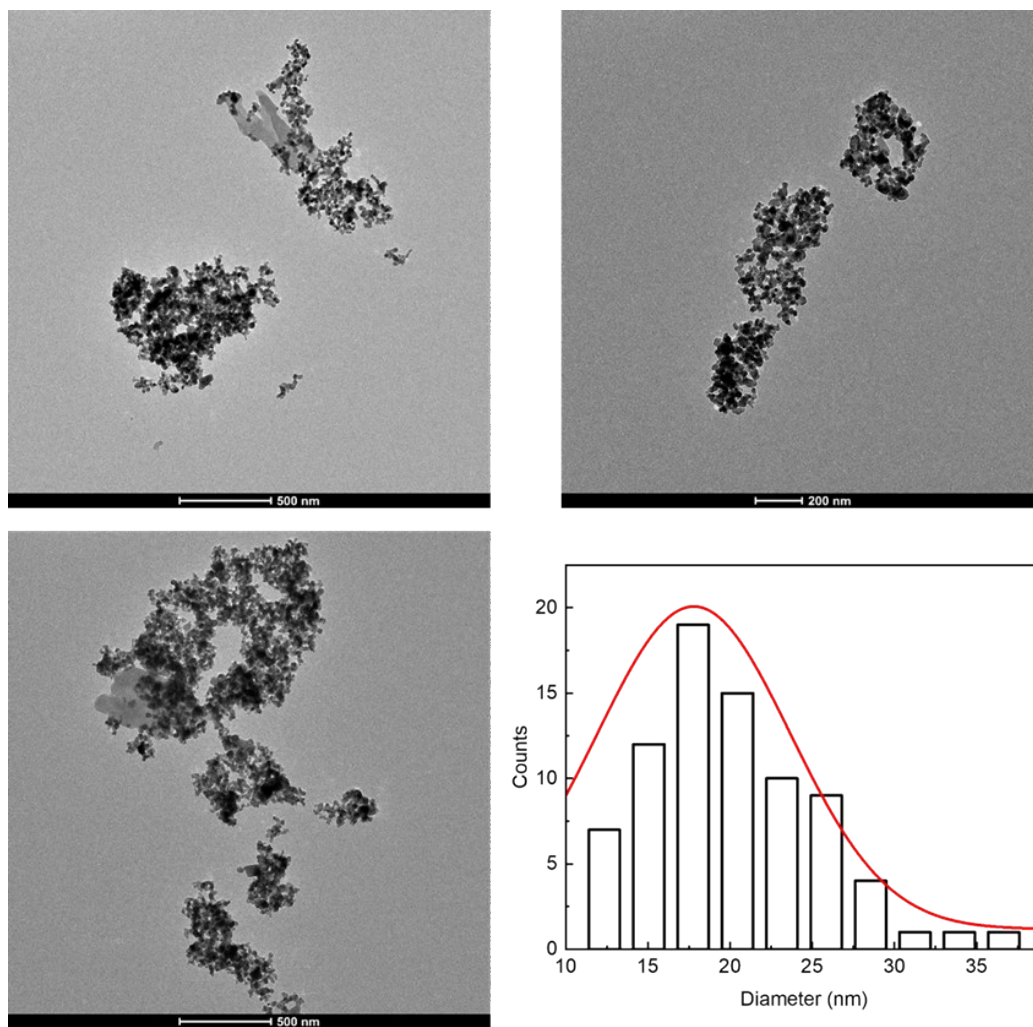


Figure S8. TEM images of $[\text{Cu}_2\text{I}_2(\text{fcSe})_2]_n@ \text{TiO}_2$ nanoparticles and size distribution.

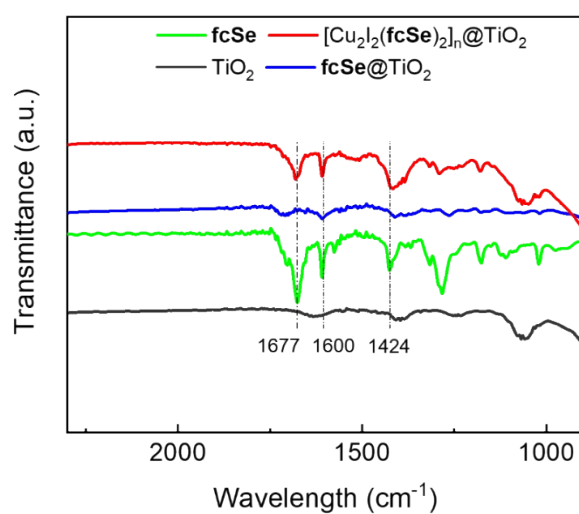


Figure S9. FTIR spectra of TiO_2 , fcSe , $\text{fcSe}@ \text{TiO}_2$ and $[\text{Cu}_2\text{I}_2(\text{fcSe})_2]_n@ \text{TiO}_2$

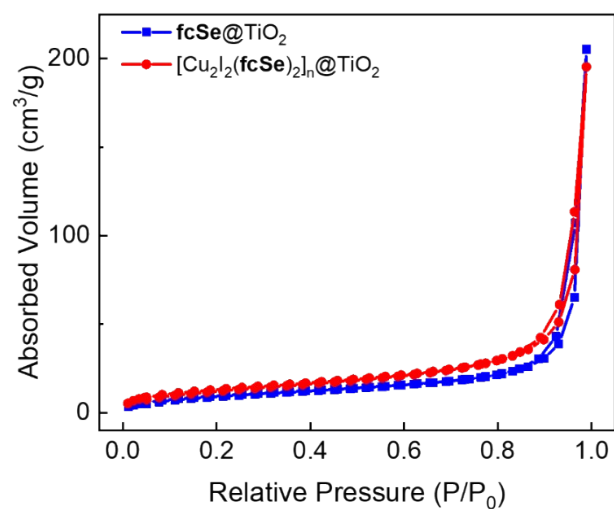


Figure S10. Nitrogen adsorption-desorption isotherms of **fcSe@TiO₂** (blue) and **[Cu₂I₂(fcSe)₂]_n@TiO₂** (red).

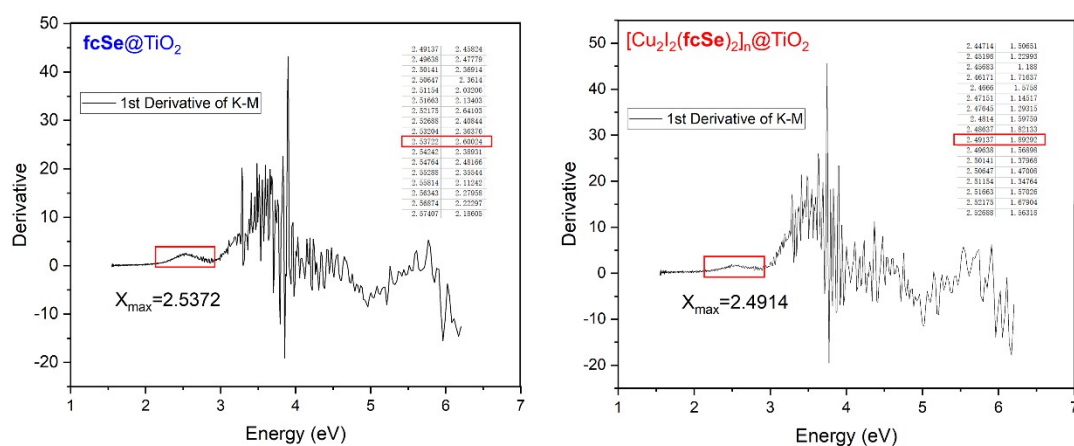


Figure S11. The first derivative of the Tauc Plot curve for **fcSe@TiO₂** and **[Cu₂I₂(fcSe)₂]_n@TiO₂**.

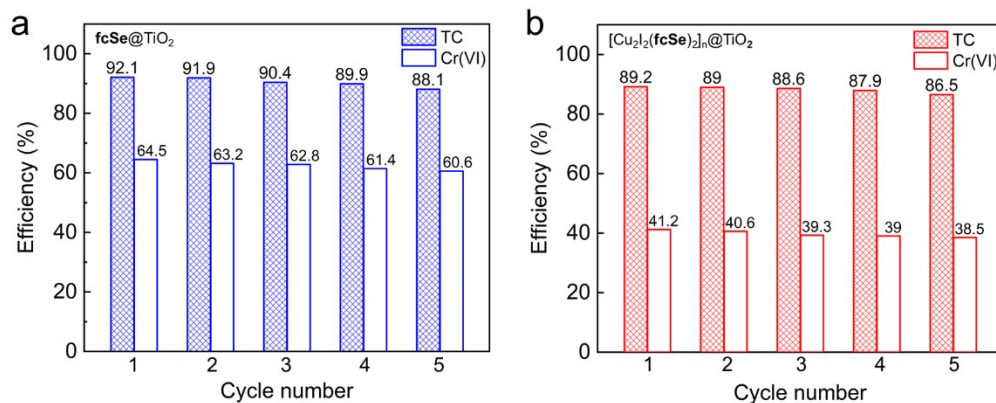


Figure S12. Transformation efficiency of (a) $fcSe@TiO_2$, (b) $[Cu_2I_2(fcSe)_2]_n@TiO_2$ for TC and Cr(VI) in multiple catalytic cycles.

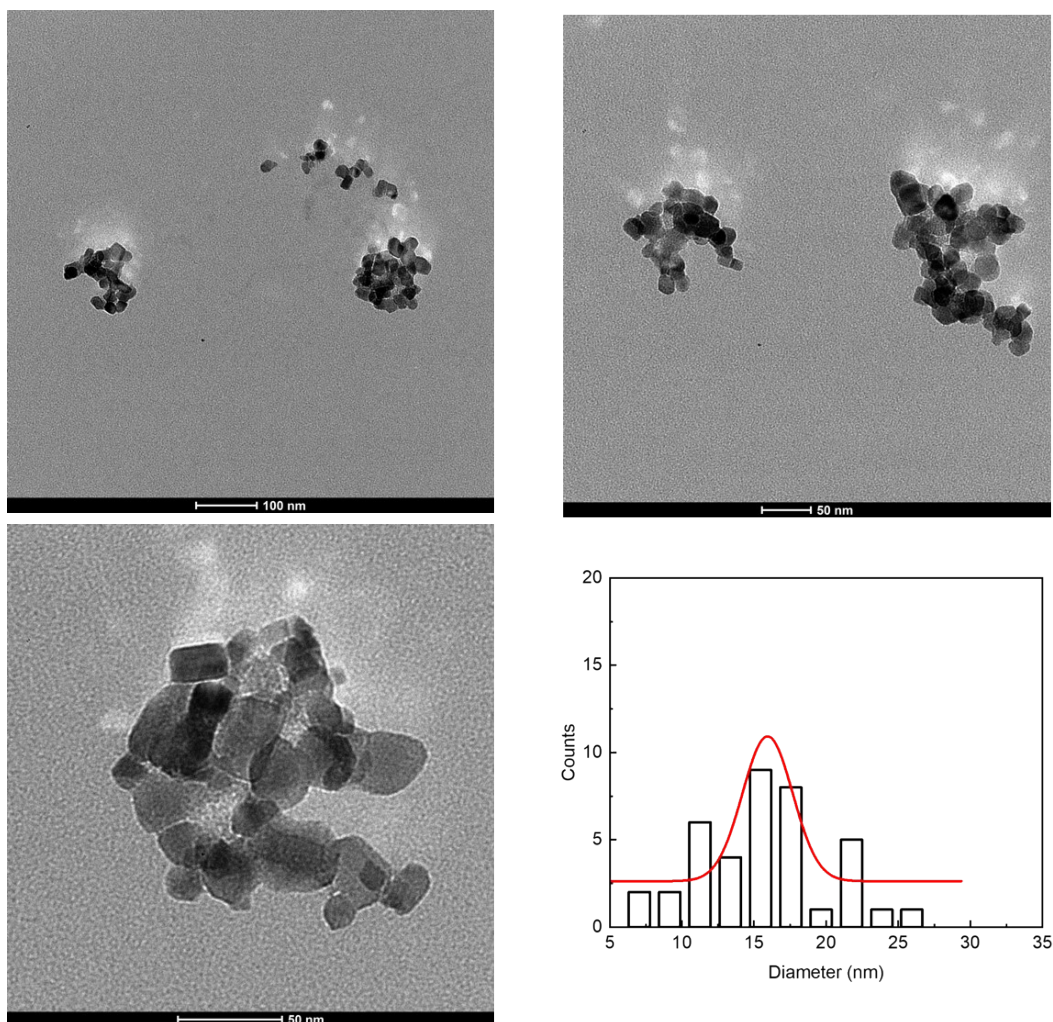


Figure S13. TEM images of $fcSe@TiO_2$ nanoparticles and size distribution after five catalytic cycles.

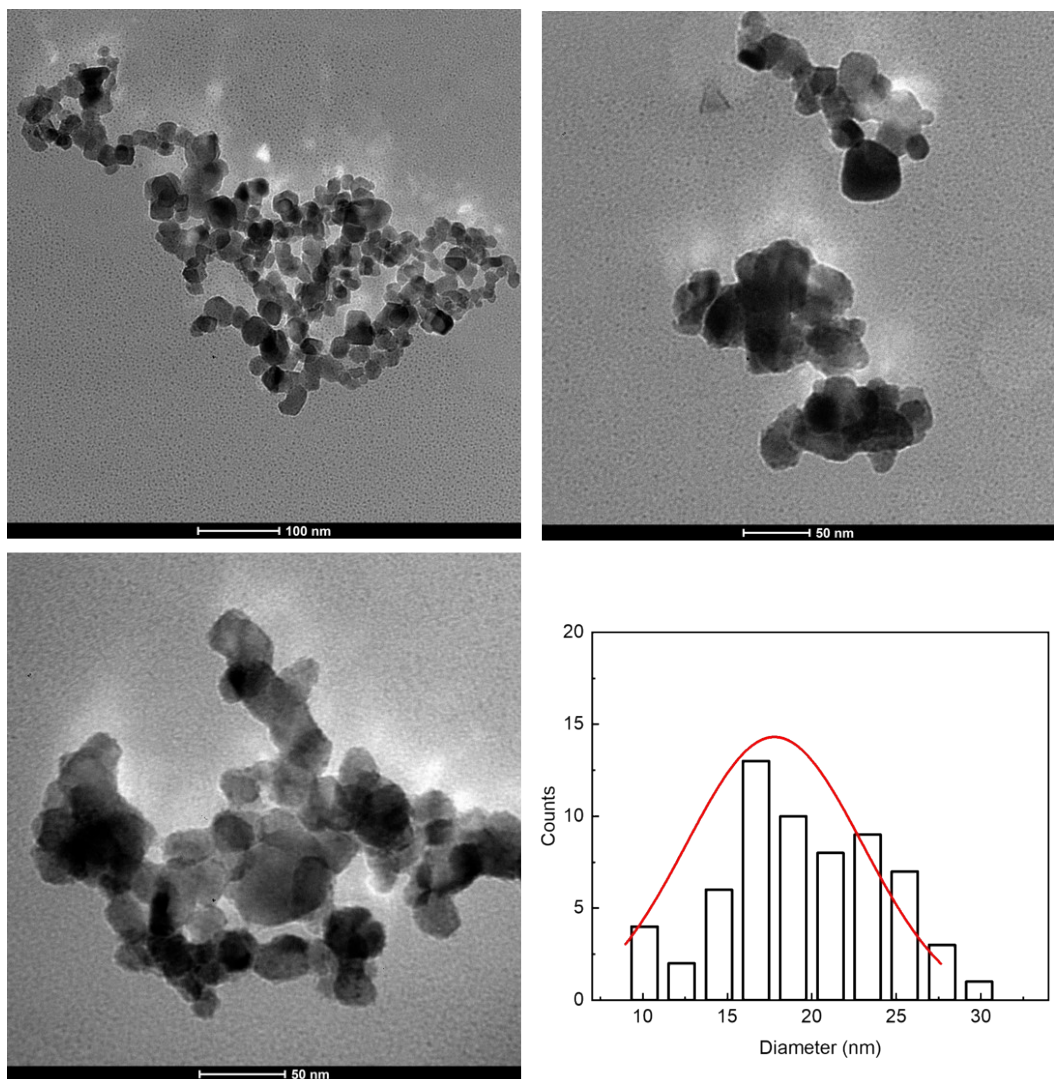


Figure S14. TEM images of $[\text{Cu}_2\text{I}_2(\text{fcSe})_2]_n@ \text{TiO}_2$ nanoparticles and size distribution after five catalytic cycles.

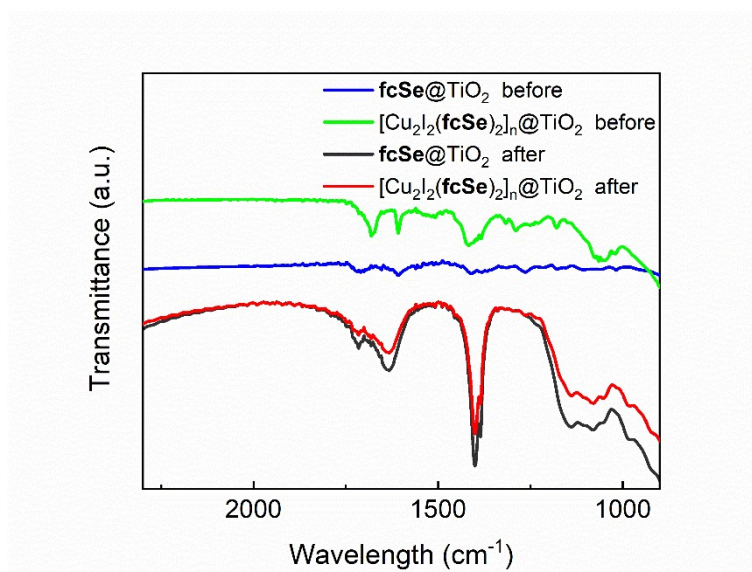


Figure S15. FTIR spectra of TiO₂, fcSe, fcSe@TiO₂ and [Cu₂I₂(fcSe)₂]_n@ TiO₂ after five cycles.

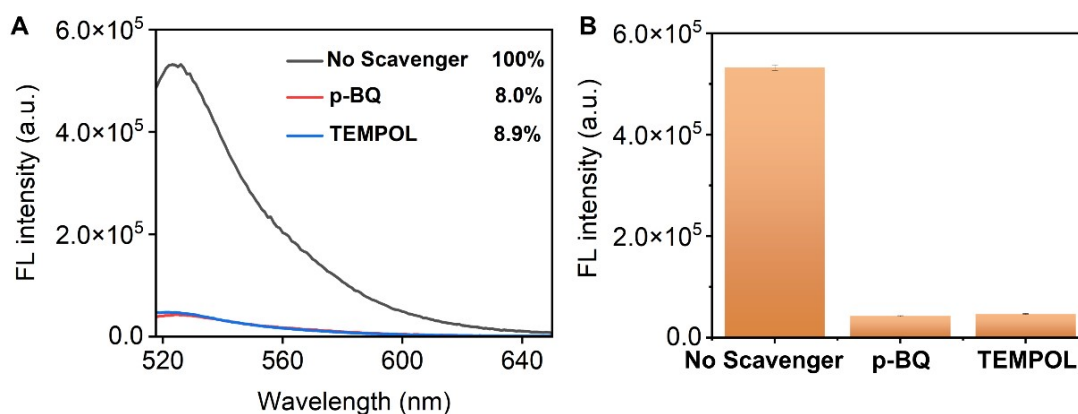


Figure S16. The fluorescence change of SOSG in response to ¹O₂ generated in the [Cu₂I₂(fcSe)₂]_n@TiO₂ system with ·O₂⁻ scavenger p-BQ (red line) or TEMPOL (blue line). Experimental conditions are 25-30 °C, pH = 7, [Cu₂I₂(fcSe)₂]_n@TiO₂ dosage = 0.2 g/L, H₂O₂ concentration = 20 mM, p-BQ or TEMPOL concentration = 2.5 mM, SOSG concentration = 0.25 μM, 5 min of visible light irradiation.

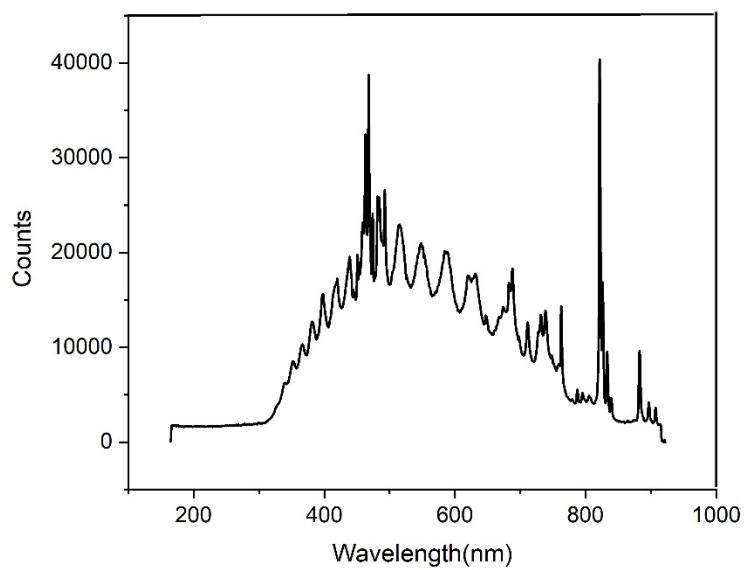


Figure S17. The spectrum of the Xenon Lamp MC-PF300C.

Table S1. Crystallographic data for **L0**

Complexes	L0
Empirical formula	C ₂₈ H ₂₆ FeO ₄ Se ₂
Formula weight	640.26
Crystal system	Monoclinic
Space group	<i>P</i> 2 ₁ / <i>c</i>
<i>a</i> (Å)	12.387(3)
<i>b</i> (Å)	6.2596(17)
<i>c</i> (Å)	33.747(9)
α (°)	90
β (°)	91.613(3)
γ (°)	90
<i>V</i> (Å ³)	2615.6(12)
<i>Z</i>	4
<i>D</i> _c (g·cm ⁻³)	1.626
μ (mm ⁻¹)	3.392
<i>F</i> (000)	1280
Crystal size (mm ³)	0.18 × 0.06 × 0.05
θ Range	1.645-25.000
Reflections collected	17262
Independent reflections	4578 [<i>R</i> _{int} = 0.0610]
Reflections observed [<i>I</i> > 2 σ (<i>I</i>)]	3384
Data/restraints/parameters	4578/316/0
Goodness-of-fit on <i>F</i> ²	1.101
<i>R</i> ₁ / <i>wR</i> ₂ [<i>I</i> > 2 σ (<i>I</i>)]	0.1038/0.1999
<i>R</i> ₁ / <i>wR</i> ₂ (all data)	0.0785/0.1908
Max., Min. $\Delta\rho$ (e·Å ⁻³)	1.663, -1.490

Table S2. Selected bond lengths (Å) and bond angles (°) for **L0**

Bond lengths		Bond lengths		Bond angles	
Se1-C1	1.921(8)	Se1-C11	1.972(8)	C1-Se1-C11	98.6(3)
Se2-C6	1.892(9)	Se2-C19	1.943(9)	C6-Se2-C19	95.4(4)
O1-C18	1.199(15)	O2-C18	1.343(17)	C18-O2-C27	117.0(11)
O3-C26	1.212(14)	O4-C26	1.327(15)	C26-O4-C28	117.2(11)

Table S3. Zeta potentials and Z-average hydrodynamic diameters of **fcSe@TiO₂** and **[Cu₂I₂(fcSe)₂]_n@TiO₂** at different pH.

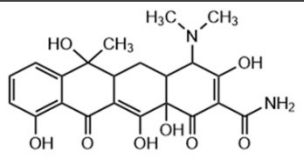
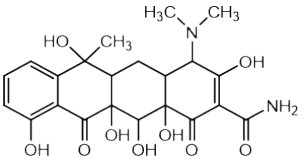
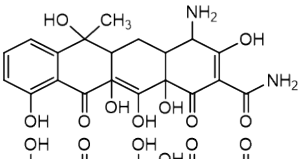
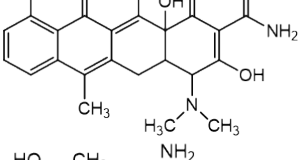
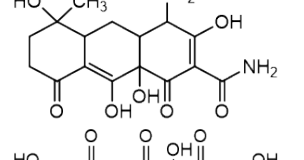
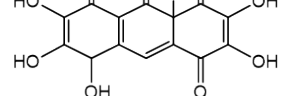
pH	fcSe@TiO₂		[Cu₂I₂(fcSe)₂]_n@TiO₂	
	ζ (mv) \pm SD	Z-average size (nm) \pm SD	ζ (mv) \pm SD	Z-average size (nm) \pm SD
3	9.07 \pm 1.0	6716 \pm 57.0	3.70 \pm 0.8	4933 \pm 32.0
5	5.06 \pm 3.6	1530 \pm 22.0	9.77 \pm 2.2	4338 \pm 63.0
7	25.3 \pm 2.0	673.3 \pm 43.0	-7.46 \pm 1.2	3141 \pm 24.0
9	-40.8 \pm 6.5	366.2 \pm 48.0	-23.1 \pm 4.3	345.4 \pm 30.0

Table S4. TC photocatalytic degradation efficiency comparison of **fcSe@TiO₂** and **[Cu₂I₂(fcSe)₂]_n@TiO₂** with other representative systems.

Catalyst	Catalyst dosage g/L	H ₂ O ₂ mM	Initial pH	TC initial concentration mg/L	Degradation effect	Reference
fcSe@TiO₂	0.2	19.8	7	20	30 min 93.1%	This work
[Cu₂I₂(fcSe)₂]_n@TiO₂	0.2	19.8	7	20	30 min 91.3%	This work
Fe ²⁺	0.005	0.59	7.5	100	60 min 97.1%	2

Fe-MOFs	0.15	10 mL/L	4.1	50	20 min 82.5%	3
C@FONC	0.5	5	3	150	180 min 97.9%	4
Fe-POM/CNNS-N _{vac}	1	10	4.5	20	18 min 96.5%	5
15-yCeO ₂ /Fh	0.4	50	4	20	60 min 93.6%	6
Fe-R-2	0.4	10	3.81	100	120 min 98.1%	7
APRM-110	0.5	20	4.3	40	60 min 87.8%	8
MFO-Au ₃	0.1	50	6	20	90 min 88.3%	9
0.8MLD/CN/Fe ₃ O ₄	0.5	80	7	20	80 min 95.8%	10
Cu-HNCN/PF	0.2	20	6.5	10	50 min 96%	11
Fe-g-C ₃ N ₄ /Bi ₂ WO ₆	0.4	1	6.5	10	120 min 93.9%	12
FMCNEP	1.3	20	5	25	60 min 97.5%	13

Table S5. LC-MS information and proposed structure of photocatalytic products in the catalytic degradation of TC by **fcSe@TiO₂** and **[Cu₂I₂(fcSe)₂]_n@TiO₂**

Intermediate Products	Retention Time (min)	MS (m/z)	Molecular Formula	Supposed Structure	fcSe@TiO ₂	[Cu ₂ I ₂ (fcSe) ₂] _n @TiO ₂
TC	6.49-6.59	445	C ₂₂ H ₂₄ N ₂ O ₈		✓	✓
I1	6.62-6.72	461	C ₂₂ H ₂₆ N ₂ O ₉		✓	✓
I2	6.77-6.86	433	C ₂₀ H ₂₂ N ₂ O ₉		✓	✓
I3	6.87-6.94	427	C ₂₂ H ₂₂ N ₂ O ₇		✓	✓
I4	6.48-6.45	353	C ₁₆ H ₂₀ N ₂ O ₇		✓	✓
I5	6.21-6.3	337	C ₁₄ H ₈ O ₁₀		✓	✓

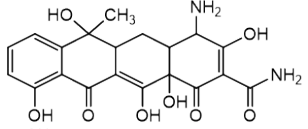
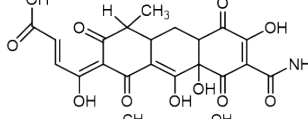
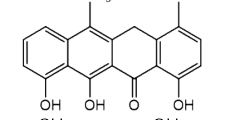
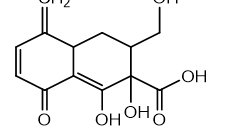
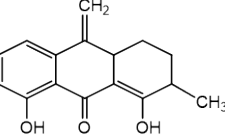
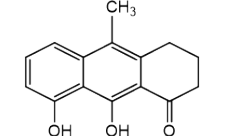
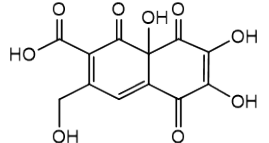
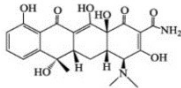
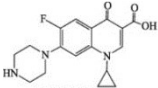
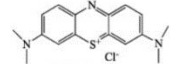
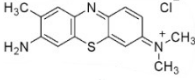
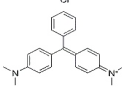
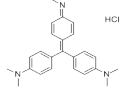
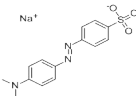
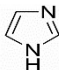
I6	7.19-7.27	417	$C_{20}H_{22}N_2O_8$		✓	✓
I7	7.04-7.11	447	$C_{20}H_{17}NO_{11}$		✓	✓
I8	7.13-7.19	325	$C_{19}H_{14}O_5$		✓	-
I9	6.8-6.91	266	$C_{13}H_{14}O_6$		✓	-
I10	6.2-6.39	256	$C_{16}H_{16}O_3$		✓	✓
I11	5.85-6.04	242	$C_{15}H_{14}O_3$		✓	✓
I12	6.73-6.82	297	$C_{12}H_8O_9$		-	✓

Table S6. Evaluation of fcSe@TiO_2 and $[\text{Cu}_2\text{I}_2(\text{fcSe})_2]_n@\text{TiO}_2$ in the visible light photo-degradation of representative N-cyclic organics^a.

N-cyclic organics	Structural formula	fcSe@TiO_2		$[\text{Cu}_2\text{I}_2(\text{fcSe})_2]_n@\text{TiO}_2$	
		Removal efficiency	$\eta_{\text{CO+HCOOH}}^b$	Removal efficiency	$\eta_{\text{CO+HCOOH}}^b$
Tetracycline		93.1%	7.2%	91.3%	6.1%
Ciprofloxacin		86.2%	11.8%	64.9%	20.8%
Methylene blue		93.9%	8.1%	41.4%	6.6%
Toluidine blue		94.2%	6.9%	88.9%	10.8%
Pigment Green		92.0%	3.0%	93.7%	4.3%
Basic violet		92.3%	4.4%	86.2%	3.7%
Methyl Orange		17.1%	7.9%	16.0%	7.3%
Imidazole		16.6%	4.7%	25.9%	5.9%

^a Experimental conditions are 25-30 °C, pH = 7, catalyst dosage = 0.2 g/L, H_2O_2 concentration = 20 mM.

^b The conversion rate CO and HCOOH $\eta_{\text{CO+HCOOH}}$ was calculated by Eq. (4).

References

- [1] M.R. Burgess, S. Jing, C.P. Morley, *J. Organomet. Chem.*, 2006, **691**, 3484-3489.
- [2] C. Han, H. Park, S. Kim, V. Yargeau, J. Choi, S. Lee, J. Park, *Water Res.*, 2020, **172**, 115514.
- [3] Q. Wu, H. Yang, L. Kang, Z. Gao, F. Ren, *Appl. Catal. B-Environ.*, 2020, **263**, 118282.
- [4] J. Zhou, F. Ma, H. Guo, D. Su, *Appl. Catal. B-Environ.*, 2020, **269**, 118784.
- [5] J. Jiang, X. Wang, Y. Liu, Y. Ma, T. Li, Y. Lin, T. Xie, S. Dong, *Appl. Catal. B-Environ.*, 2020, **278**, 119349.
- [6] X. Huang, N. Zhu, F. Mao, Y. Ding, S. Zhang, H. Liu, F. Li, P. Wu, Z. Dang, Y. Ke, *Chem. Eng. J.*, 2020, **392**, 123636.
- [7] S. Guo, W. Yang, L. You, J. Li, J. Chen, K. Zhou, *Chem. Eng. J.*, 2020, **393**, 124758.
- [8] Q. Li, G. Wei, Y. Yang, L. Gao, L. Zhang, Z. Li, X. Huang, J. Gan, *Chem. Eng. J.*, 2021, **424**, 130537.
- [9] L. Qin, Z. Wang, Y. Fu, C. Lai, X. Liu, B. Li, S. Liu, H. Yi, L. Li, M. Zhang, Z. Li, W. Cao, Q. Niu, *J. Hazard Mater.*, 2021, **414**, 125448.
- [10] X. Zhang, B. Ren, X. Li, B. Liu, S. Wang, P. Yu, Y. Xu, G. Jiang, *J. Hazard Mater.*, 2021, **418**, 126333.
- [11] X. Zhang, B. Xu, S. Wang, X. Li, C. Wang, Y. Xu, R. Zhou, Y. Yu, H. Zheng, P. Yu, Y. Sun, *Appl. Catal. B-Environ.*, 2022, **306**, 121119.
- [12] C. Liu, H. Dai, C. Tan, Q. Pan, F. Hu, X. Peng, *Appl. Catal. B-Environ.*, 2022, **310**, 121326.
- [13] Y. Liu, X. Wang, Q. Sun, M. Yuan, Z. Sun, S. Xia, J. Zhao, *J. Hazard. Mater.*, 2020, **424**, 127387.